

# Super-resolution study of Wall Sheer Stress in cerebral aneurysm with AI PIV

Marta Sobkowiak<sup>1\*</sup>, Marek Ples<sup>1\*</sup>, Wojciech Wolański<sup>1</sup>, Runjie Wei<sup>2</sup>, Wojciech Majewski<sup>2</sup>, Wojciech Kaspera<sup>3</sup>

1: Silesian University of Technology, Gliwice, Poland

2: Microvec Pte Ltd, Singapore

3: Medical University of Silesia, Sosnowiec, Poland

\* Correspondent authors: [m\\_sobkowiak@outlook.com](mailto:m_sobkowiak@outlook.com), [marek.ples@o2.pl](mailto:marek.ples@o2.pl)

**Keywords:** CFD, PIV, AI PIV, fluid mechanics, cerebral aneurysm

## ABSTRACT

Aneurysms are one of the most common unexplored causes of death. There are many studies conducted by scientists around the world on this issue. The main problem raised is the cause of aneurysms [17]. Here, the division includes several branches, i.e. genetic conditions, lifestyle, eg. smoking, and finally hemodynamic factors of blood flow [4, 10, 13]. It is well known that the aneurysm is formed and ruptured at the site of high wall shear stress (WSS). This paper presents the comparison of results of CFD blood flow simulations with experimental values obtained with the Particle Image Velocimetry (PIV) method in a 3D model of a cerebral aneurysm. A 3D model of a cerebral aneurysm was developed using specific patient CT data. The hemodynamical parameters were analysed for different flow rates in a 3D model under pulsatile flow conditions. The CFD simulation was done using Ansys CFX software. Results of the simulation were validated with the experimental PIV method. Two different PIV methods were employed: traditional PIV based on cross-correlation (CC) algorithms and Artificial Intelligence PIV (AI PIV) based on Deep Learning and Convolutional Neural Networks. The obtained results showed a better correlation between CFD simulation and types of PIV analysis for data of AI PIV, which allows for a much higher spatial resolution of the resulting velocity field. Analysis of the results was promising and showed that AI PIV could be used to get accurate results.

---

## 1. Introduction

An intracranial aneurysm, also known as a brain aneurysm, is a cerebrovascular disorder in which weakness in the wall of a cerebral artery or vein causes a localized dilation or ballooning of the blood vessel. They are more common in women than in men, most often between the ages of 30 and 60 [17]. People with certain hereditary diseases are also at a higher risk. Most cerebral aneurysms do not show symptoms until they either become very large or rupture. Small unchanging brain aneurysms are usually asymptomatic. Larger aneurysms that continue to grow can compress other tissues and cause damage to nerves, such as: numbness, paralysis on one side of the face, vision changes or double vision, pain above and behind the eye, weakness, a dilated pupil in the eye [17]. Computational Fluid Dynamics (CFD) and the analysis of blood flow through the cerebral vessels help analyze this problem. Using the specialized CFD software, the

phenomenon of blood flow in the aneurysm is examined, and the hemodynamic parameters on the artery wall, such as shear stress and pressure are determined. CFD is used by many specialized commercial programs such as Ansys Fluent, Ansys CFX, Autodesk CFD, as well as free ones such as simFlow. Thanks to these tools, it is possible to verify which hemodynamic parameters influence the formation and rupture of aneurysms. On the other hand, based on morphometric parameters, it can be predicted whether in the future a particular artery may weaken the arterial wall at its bifurcation, which may further result in the formation of a brain aneurysm [12]. In order to verify numerical simulations, Particle Image Velocimetry (PIV) tests on phantoms of geometric artery models are often used. These studies allow us to assess the quality of numerical analysis and the degree of accuracy of mapping the real conditions of this analysis. Such studies and comparisons have been done, for example, by Vlachos et al [2]. Thanks to these verifications, it is also possible to determine whether the given numerical simulation settings can serve as a reliable model for physicians, for example, to assess the risk of an aneurysm occurrence or rupture [15].

Particle Image Velocimetry (PIV) is a technique which has been used in fluid mechanics since 1984. The first paper that used the term and defined the concept of PIV was published by Adrian [1] and Pickering and Halliwell [9]. The methodology behind PIV involves the use of a laser light, converted to a light sheet, to illuminate the seeding particles introduced into the flow. The particles with a density similar to the flow medium follow the flow with a high level of accuracy. The light scatters off the particles and a camera captures an image pair within a very short period of time. These two images, showing the light scattering off the particles, are processed using a CC technique. During this process, the images are divided into a grid of small interrogation windows (IW) which are then used to calculate a fluid velocity vector using the direction and speed. By combining these single vectors into a velocity field, the resulting velocity vector field displays the characteristics of the flow. In the 1990s, the era of Digital PIV (DPIV) began with the introduction of digital cameras based on CCD sensors. Research from Willert and Gharib [14] showed promising results, despite the low resolution of the first digital cameras. DPIV has been proven to be accurate enough to offer good results. Since then, the resolution of the digital cameras has not been an issue. Nowadays digital cameras with resolutions of up to 50 megapixels are used for PIV. As mentioned above, the PIV system captures an image pair showing the particles scattering light and then analyses the particle displacement of the two images by using a CC algorithm. Currently, the most common method is the multigrid iterative calculation based on image deformation [11]. The algorithm reduces the IW size step by step, starting from  $64 \times 64$  pixels, through  $32 \times 32$ , and down to  $16 \times 16$  pixels with the number of vectors quadrupling each time (Figure 1). This increases

the velocity field resolution results into a higher precision velocity field. Most traditional commercial and free PIV software packages are based on this model.

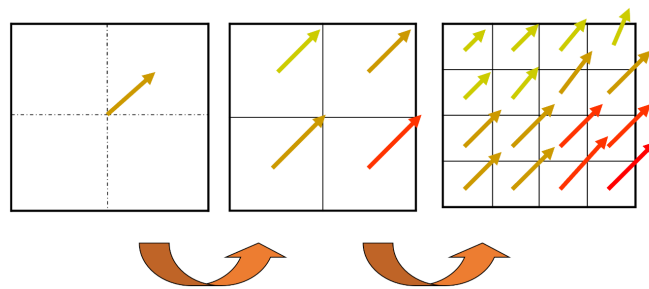


**Fig. 1** Velocity vector fields with IW of 64x64, 32x32 and 16x16 pixels

However, there is a limit. If the IW becomes smaller than 16x16 pixels, the difficulty of correlating the image pairs increases and the uncertainty of the calculation becomes larger as well. This leads to one of the main issues in PIV: spatial resolution limitation. Many small flow details will not be visible.

Recent research on Deep Learning and Convolutional Neural Networks and how it can be applied to PIV has led to the introduction of the first AI PIV software modules [8]. Based on Convolutional Neural Networks, the software allows analysis that is no longer limited by the size of the IW. The spatial resolution limitation is eliminated and generates the velocity vector field with a resolution down to a one-pixel level for an instantaneous flow field, assuming that the acquired image quality allows for it. Therefore, the resulting super-resolution becomes a major benefit from deep learning in fluid mechanics [5, 6]. As shown on Figure 2, AI PIV allows velocity vectors to be accurately calculated for IW equivalents with much smaller grid sizes, down to a one-pixel level.

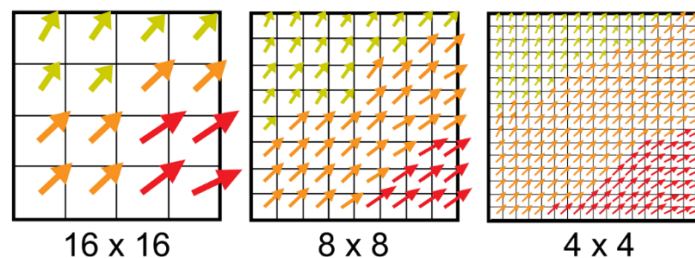


**Fig. 2** Velocity vector fields obtained with AI PIV shown in IW form

The idea behind AI PIV was to design a deep learning estimator for fluid motion. This convolutional neural network is a mapping function between images and motion. The input is the same as in CC PIV: an input of an image pair and an output of a velocity field [3]. The optical flow

computation was used as a principle and deep learning was then added to create a deep learning motion estimator. Optical flow computation normally relies on the optimization of an objective function and provides dense motion fields for the entire image while the motion fields obtained by CC based PIV are sparse.

The goal of this study is to compare traditional CCPIV and AI PIV data with CFD simulation blood flow through the cerebral vessel with an aneurysm. The authors analyze how the modality and spatial resolution affect flow through the aneurysm vessel.

## 2. Material and method

The CFD simulation using PIV and AI PIV analysis of blood flow through the cerebral vessel with an aneurysm was done for the same geometrical model. The 3D model of a vessel with an aneurysm was developed based on specific patient CT data (Figure 3a) using Mimics software (Materialise, Belgium). The first type of the model was based on the actual patient data which has been simplified. This simplified model has been used for numerical and experimental studies. Using real morphometric values of the patients' vessel (Figure 4a), the diameter of the inlet was 4.7 mm, with outlets of – 4 mm and 3.7 mm which fulfill Murray's law [7].

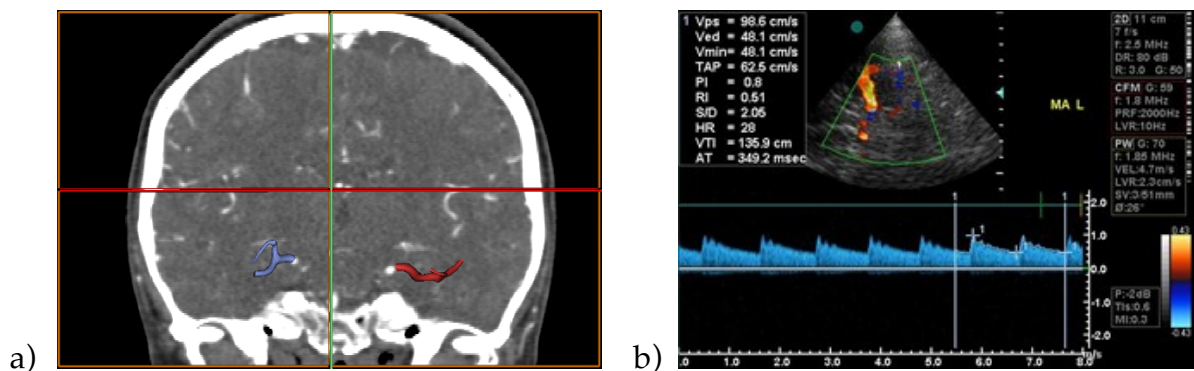


**Fig. 3** a) The segmented cerebral vessels from CT data, b) doppler ultrasound image

The next step was to develop a numerical model of the flow through the designed vessel. The real values of the flow velocity were determined during a Doppler ultrasound examination (Figure 3b). The obtained speed profile was implemented into CFD simulations at the inlet of the model. A constant pressure of 0 Pa was set at the model outputs. The type of the flow was set to laminar due to the Reynolds number not exceeding 1000 [16]. Blood was simulated as a non-Newtonian fluid using the Bird-Carreau model. The following mechanical properties of the fluid were assumed: molar mass - 18.02 kg/kmol, density - 2.1 g/cm<sup>3</sup>, heat capacity - 4181.7 J/kg\*K,

temperature - 37°C, viscosity - 0.003 Pa\*s. The number of elements in mesh was about 80,000 nodes – 30,500 and the element size was 0.06 mm (Figure 4b).

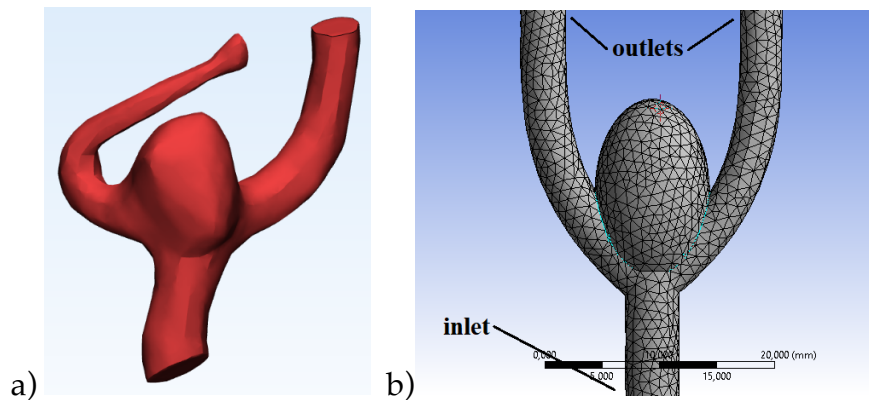


**Fig. 4** a) Real model taken from CT scans, b) geometric model of cerebral vessel with aneurysm

The designed geometric model was printed on a 3D printer and then poured with the appropriate material using a method unique to this study. In this way, a phantom of the vessel was obtained and then used on a laboratory stand for flow analysis using the PIV method (Figure 5).

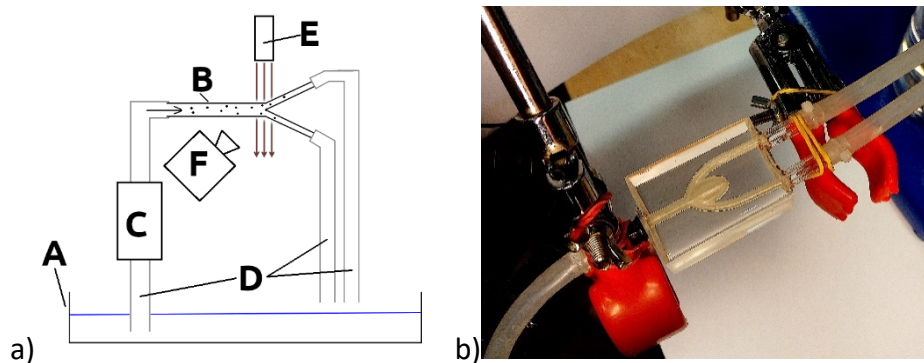


**Fig. 5** a) Scheme of the laboratory stand, b) the phantom of a cerebral aneurysm

The PIV laboratory stand includes (Figure 5): **A** – fluid reservoir, **B** – phantom of a vessel, **C** - peristaltic pump (25 rpm - rotations per minute), **D** – pipes, **E** - 2W continuous wave laser with a wavelength of 532 nm equipped with light sheet optics, where the light sheet illuminates the center plane of the phantom, **F** - CMOS camera placed above the phantom of the vessel and positioned perpendicular to the illuminated plane (maximum resolution 640x480 pixels, up to 800fps – frames per second). As a fluid medium in a PIV experiment, a sodium iodide solution in distilled water (saturated at 25°C) was used to match the refractive index of the model. The images of flow in the aneurysm were taken using MicroVec miniPIV software (Microvec Pte Ltd, Singapore) (Figure 6a) and evaluated with MicroVec miniPIV and Microvec AI PIV software modules.

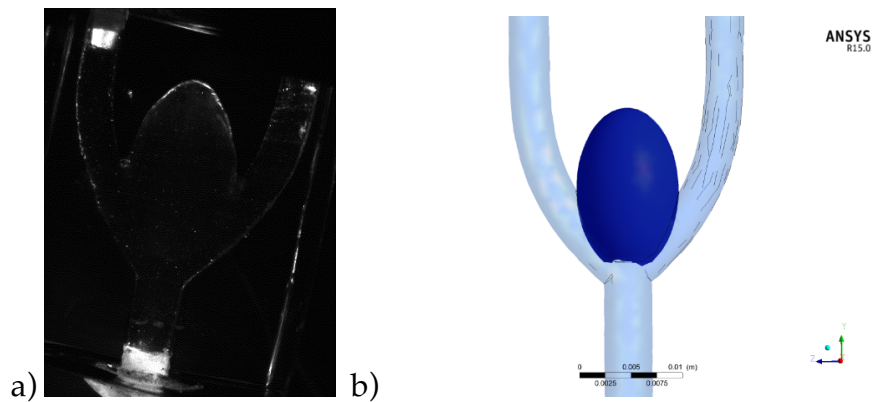


**Fig. 6** a) Example of the phantom image taken using MicroVec Mini software, b) the same view the area of CFD analysis in Ansys CFX

A few simulations were done which were intended to match each of the PIV methods used in calculating experimental results. Two traditional cross correlation settings were used with an IW of 32x32 pixel (CC PIV 32x32) and an IW of 16x16 pixels, (CC PIV 16x16). Three different AI PIV settings were used to calculate a maximum of one velocity vector per 8x8 pixels (AI PIV 8x8), 4x4 pixels (AI PIV 4x4), and 2x2 pixels (AI PIV 2x2). The area of interest, i.e. the center of the aneurysm, had a diameter of 180 pixels on the images acquired with the camera. With an actual diameter of 9 mm, the results translated to a spatial resolution of 20 pixels per millimeter or 50 microns per pixel. The second type of model was the real one (Figure 7). The whole procedure was the same as with the first phantom which was described previously.

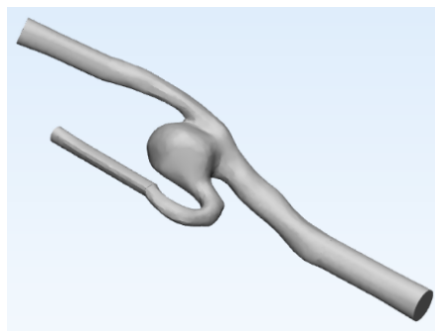


**Fig. 7** Real model of the MCA with the aneurysm visualised in the Mimics program

The average speed value from the PIV analysis was obtained at the inlet of the model during CFD simulations. Using a super-resolution AI PIV algorithm with a dense velocity field down to one pixel, increased the accuracy of WSS results (Figure 8b). It allowed for the comparison of the



values of shear stresses on the wall inside the aneurysm. Calculations of WSS values from the experiment were made in the Tecplot program (Figure 8a).

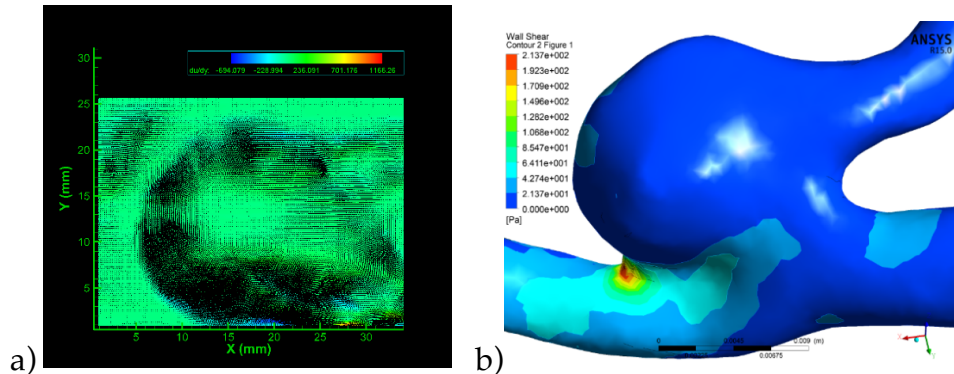


**Fig. 8** a) Experimental and b) numerical WSS results

### 3. Results

Data with different settings collected in the MicroVec miniPIV software and analyzed with MicroVec miniPIV and Microvec AI PIV software modules gave various results (Figure 9). The captured images show a clearly increasing resolution of the calculated velocity vector field. The obtained results provide a good background for the verification of the CFD simulation.

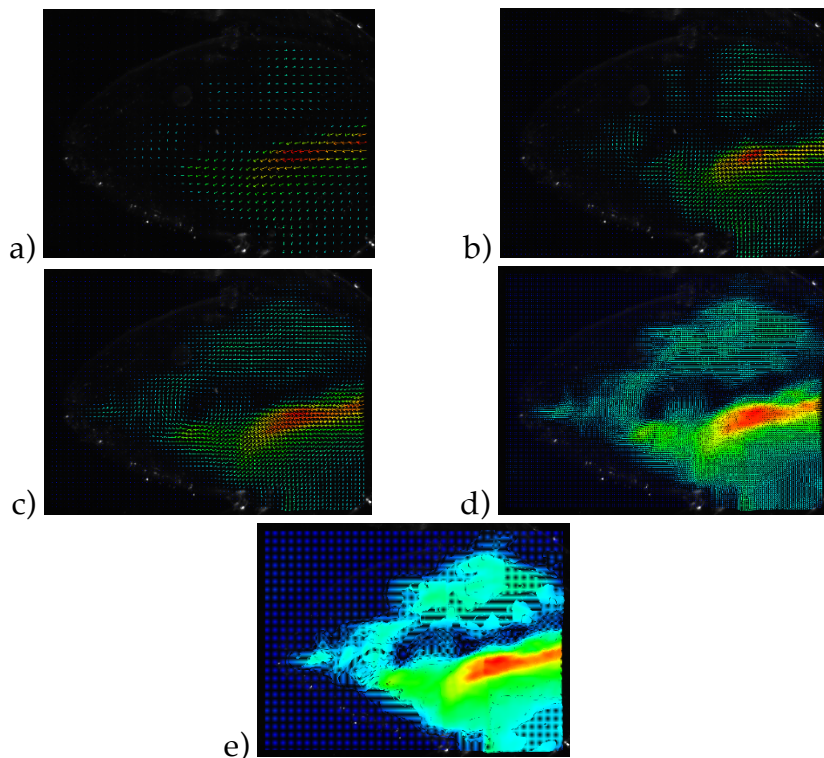


**Fig. 9** Results of PIV analysis using different types of settings: a) CC PIV 32x32, b) CC PIV 16x16, c) AI PIV 8x8, d) AI PIV 4x4, e) AI PIV 2x2

The velocity values obtained in Ansys CFX on the plane in the aneurysm (Figure 10) represented the same analyzed plane for the vectors' velocity values calculated in the MicroVec miniPIV software on the PIV laboratory stand (Figure 6). The velocity profiles obtained in the PIV experiment were compared with the results of numerical simulations carried out in the Ansys CFX program (Figure 9-11).

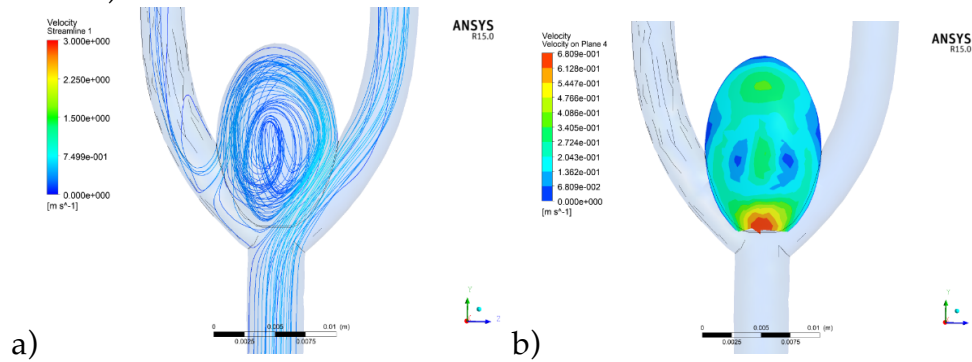
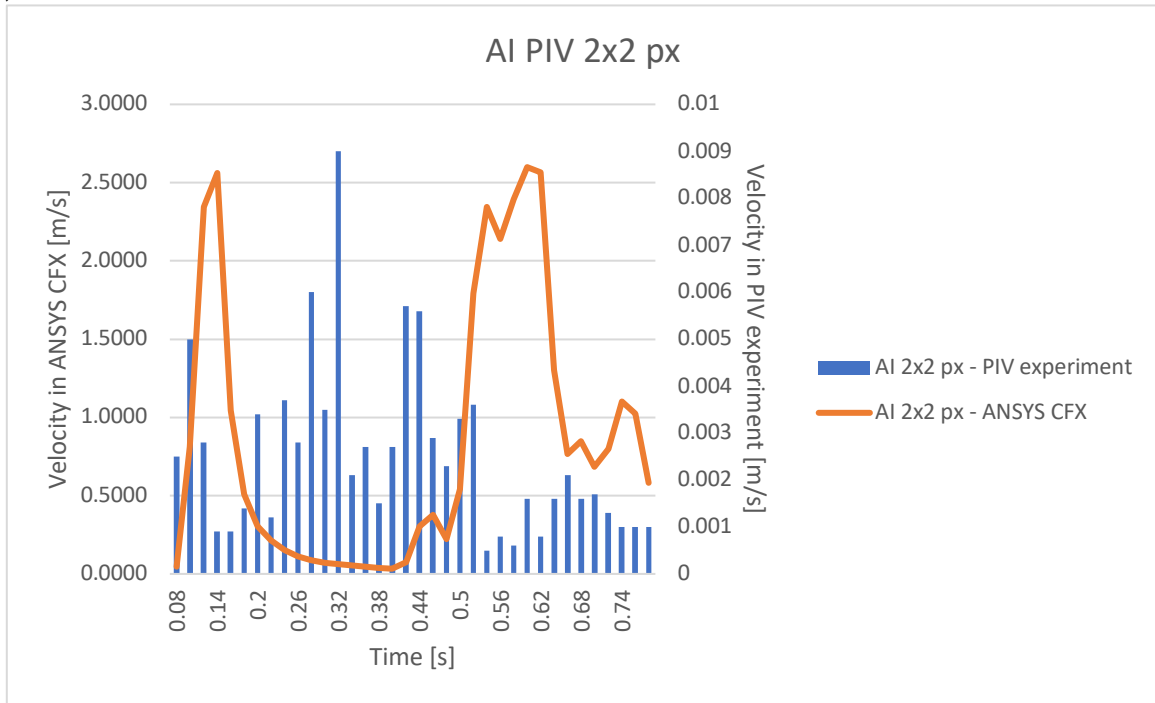


**Fig. 10** a) Ansys CFX results: particle flow in a specific model, b) plane with values of velocity

The algorithm used in the CC PIV method under the given conditions determines an insufficient amount of output data (velocity vectors) to verify the results with the data from numerical analyses. The AI PIV algorithm, on the other hand, due to its higher spatial resolution, allows for a much more accurate comparison of the obtained data.



a)



b)

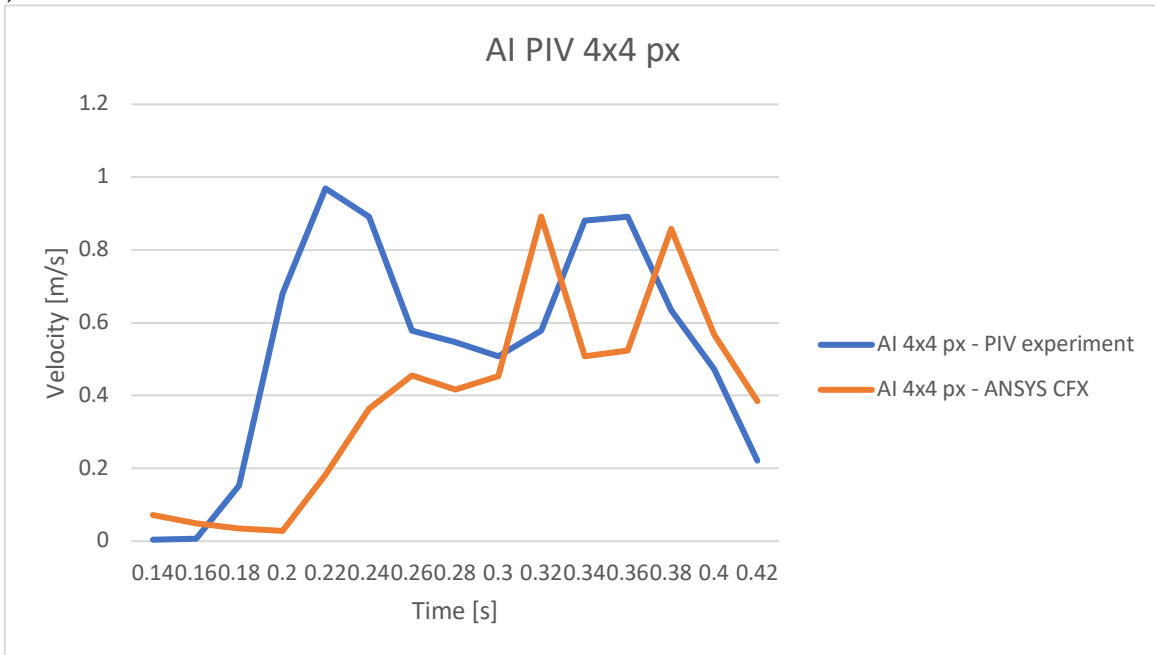


**Fig. 11** Results of the velocity values from experimental and numerical analysis using the PIV method: a) AI PIV 2x2 px, b) AI PIV 4x4 px

a)

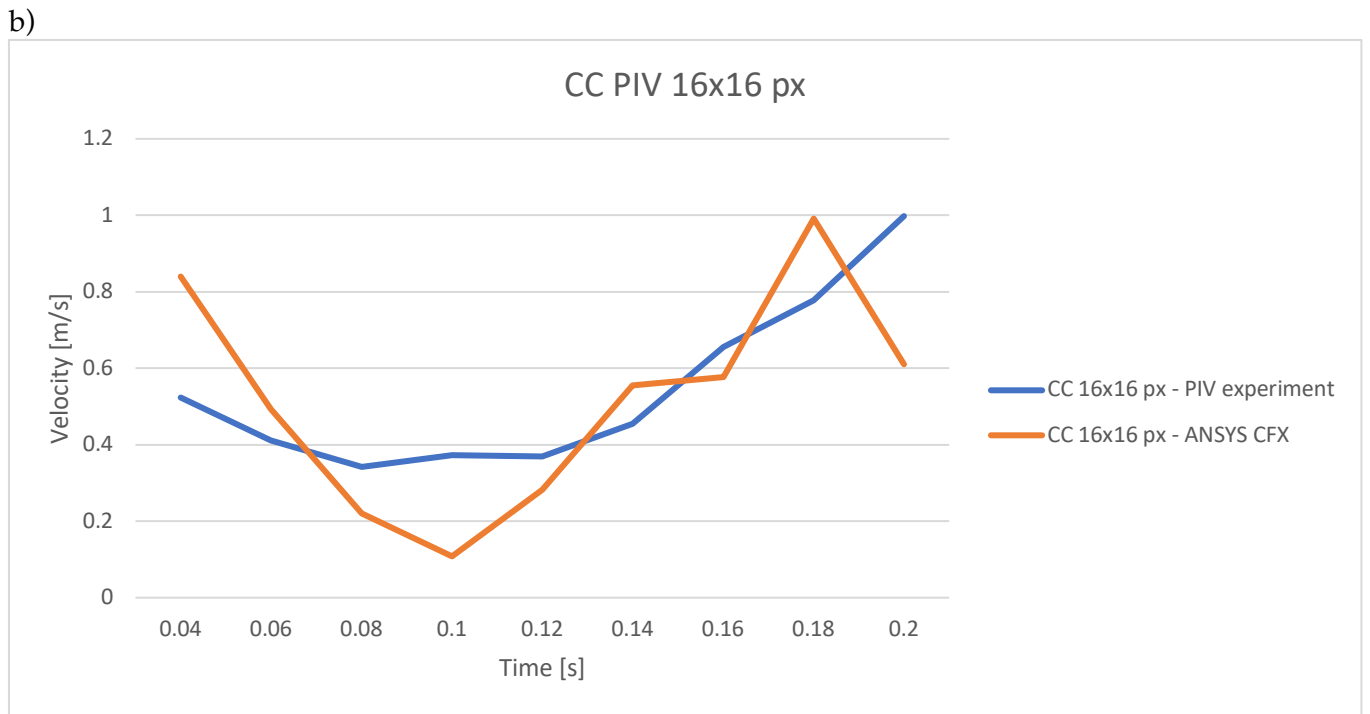
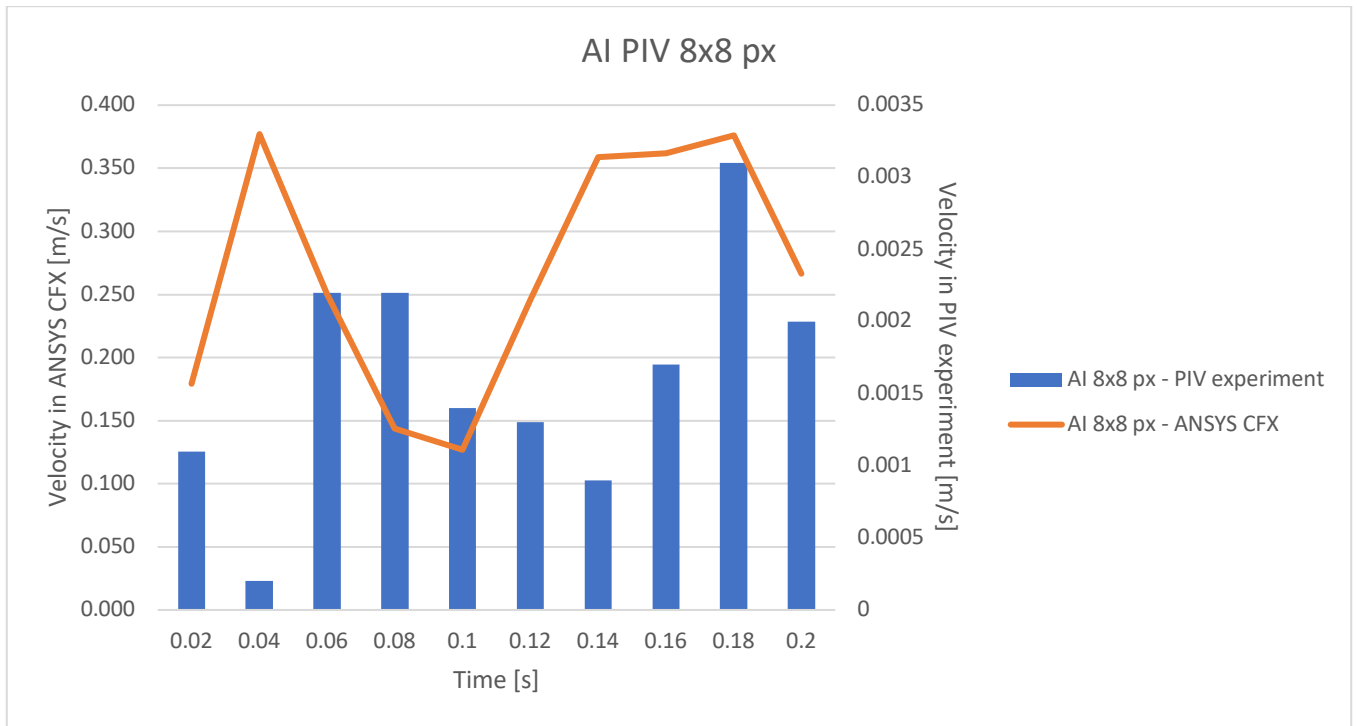


**Fig. 12** Results of the velocity values from experimental and numerical analysis for the PIV method: a) AI PIV 8x8 px, b) Cross Correlation PIV 16x16 px

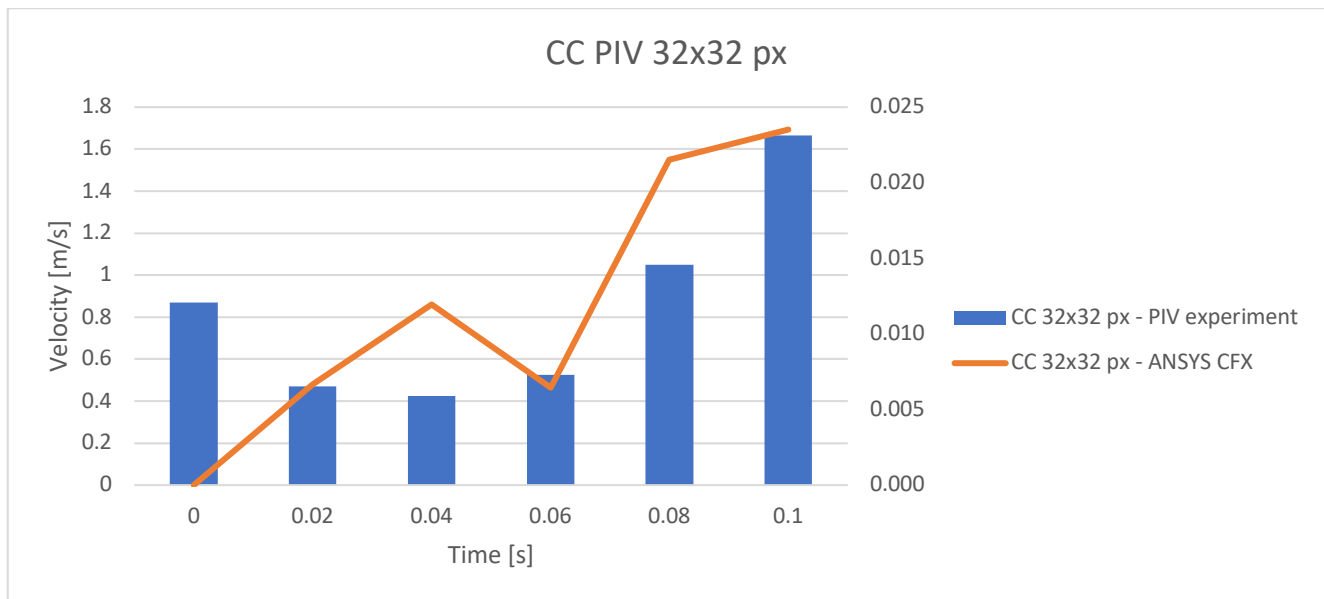


**Fig. 13** Results of the velocity values from experimental and numerical analysis using CC PIV 32x32 px method

The preliminary obtained simulation results were used to find a correlation between CFD simulation and different types of PIV analysis. The experimental results for the data of AI PIV 4x4 px (Figure 11b) had a much better correlation than the experimental results obtained using other settings, including: AI PIV 2x2 px (Figure 11a), AI PIV 8x8 px and CC PIV 16x16 px (Figure 12) or CC PIV 32x32 px (Figure 13).

In these cases, the differences in values obtained in numerical simulations and those measured using MicroVec miniPIV and AI software had one or even two orders of magnitude. The results of AI 4x4 px seems to be the optimal setting for this type of flow that allows the captured images to attain the most accurate results.

The WSS values on the top of the aneurysm calculated from the PIV analysis in the aneurysm near the wall are of the order of 52 Pa. The results of numerical simulations in the same area show the WSS values of 60 Pa (Figure 8).

### 3. Conclusion

Preliminary results of experimental studies and numerical analysis are encouraging and indicate that the best results are obtained using the PIV AI 4x4 px method (Figure 11), which theoretically has 16 times higher resolution than CC PIV method. The number of elements on the determined plane in the Ansys CFX program is approximately 60,000, and in the PIV analysis – approximately 60,000 px for the actual aneurysm area. Based on these data and the size of one element, it can be concluded that when designing a computer simulation as well as an experimental setup, these

parameters should be taken into account. More research into flows is needed to determine how much more effective the AI PIV method can be and how much more accurate it can be with the CFD simulations. These results also show that in order for the AI PIV method to obtain highly accurate dense velocity fields to validate the CFD simulation results, good quality images need to be acquired. In order to do that, some of the image acquisition challenges need to be overcome. For example, by using fluid with the same refractive index as the transparent material of the aneurysm phantom, the glare from the laser light would need to be reduced. This would allow for the capturing of images with better tracing particle distribution and better insight into the near wall layers, resulting in the experiment obtaining an even more accurate experimental representation of the flow. Increasing the resolution of the camera would be another method of improving the results.

## References

- [1] Adrian, R. J. (1984). Scattering particle characteristics and their effect on pulsed laser measurements of fluid flow: speckle velocimetry vs particle image velocimetry. *Appl. Opt.* 23, 1690-1691.
- [2] Brindise, M., Rothenberger, S., Dickerhoff, B., Schnell, S., Markl, M., Saloner, D., Rayz, V., & Vlachos, P. (2019). Patient-Specific Cerebral Aneurysm Hemodynamics: Comparison of in vitro Volumetric Particle Velocimetry, Computational Fluid Dynamics (CFD), and in vivo 4D Flow MRI, in vitro volumetric particle velocimetry and in silico computational fluid dynamics. *J. R. Soc. Interface*.
- [3] Cai, S., Zhou, S., Xu, C., & Gao, Q. (2019). Dense motion estimation of particle images via a convolutional neural network. *Experiments in Fluids*, 60:73.
- [4] Chalouhi, N., Ali, M. S., Starke, R. M., Jabbour, P. M., Tjoumakaris, S. I., Gonzalez, L. F., Rosenwasser, R. H., Koch, W. J., & Dumont, A. S. (2012). Cigarette smoke and inflammation: Role in cerebral aneurysm formation and rupture. In *Mediators of Inflammation* (Vol. 2012).
- [5] Erichson, N. B., Mathelin, L., Yao, Z., Brunton, S. L., Mahoney, M. W., & Kutz, J. N. (2020). Shallow neural networks for fluid flow reconstruction with limited sensors. *Proceedings of the Royal Society A*, 476(2238):20200097.
- [6] Fukami, K., Fukagata, K., & Kunihiro, T. K. (2019). Super-resolution reconstruction of turbulent flows with machine learning. *Journal of Fluid Mechanics*, 870:106–120.
- [7] Kaspera, W., Ćmiel-Smorzyk, K., Wolański, W., Kawlewska, E., Hebda, A., Gzik, M., & Ładziński, P. (2020). Morphological and Hemodynamic Risk factors for Middle cerebral Artery Aneurysm: a case-control Study of 190 Patients. *Scientific RepoRtS* , 10:2016.

- [8] Majewski, W., Wei, R., & Kumar, V. (2020). Developing particle image velocimetry software based on a deep neural network. *Journal of Flow Visualization and Image Processing*, 27(4): 359-376.
- [9] Pickering, C. J. D., & Halliwell, N. A. (1984). Laser speckle photography and particle image velocimetry: photographic film noise. *Appl. Opt.* 23, 2961-2969.
- [10] Sasaki, T., Kakizawa, Y., Yoshino, M., Fujii, Y., Yoroi, I., Ichikawa, Y., Horiuchi, T., & Hongo, K. (2019). Numerical Analysis of Bifurcation Angles and Branch Patterns in Intracranial Aneurysm Formation. *Clinical Neurosurgery*, 85(1), E31–E39.
- [11] Scarano, F. (2002). Iterative Image Deformation Methods in PIV. *Meas. Sci. Technol.*, vol. 13, no. 1, pp. 1–19.
- [12] Sobkowiak, M., Wolański, W., Zimny, M., Gzik, M., & Kaspera, W. (2019). Analysis of an impact of hemodynamic parameters in relation to variable morphometric features of the middle cerebral artery (MCA). In E. Tkacz, M. Gzik, Z. Paszenda, & E. Piętka, E. Tkacz, M. Gzik, Z. Paszenda, & E. Piętka (Red.), *Innovations in biomedical engineering: IBE 2018* (pp. 200–209)
- [13] Vlák, M. H. M., Rinkel, G. J. E., Greebe, P., & Algra, A. (2013). Independent risk factors for intracranial aneurysms and their joint effect: A case-control study. *Stroke*, 44(4), 984–987.
- [14] Willert, C. E., & Gharib, M. (1991). Digital particle image velocimetry. *Experiments in Fluids* 10, 181–193.
- [15] Wolański, W., Gzik-Zroska, B., Jozsko, K., Kawlewska, E., Sobkowiak, M., Gzik, M., & Kaspera, W. (2018). Impact of Vessel Mechanical Properties on Hemodynamic Parameters of Blood Flow. In *Innovations in Biomedical Engineering, Proceedings IiBE 2017*, Eds. Marek Gzik, Ewaryst Tkacz, Zbigniew Paszenda, Ewa Piętka, Cham: Springer, 271-278.
- [16] Wolański, W., Sobkowiak-Pilorz, M., Ples, M., Kawlewska, E., & Kaspera, W. (2020). Effect of radius changes of middle cerebral artery (MCA) on hemodynamic parameters. In V. Fuis, V. Fuis (Red.), *Engineering mechanics 2020: 26th International conference, Brno, Czech Republic, November 24-25, 2020* (pp. 536–539). Institute of Thermomechanics of the Czech Academy of Sciences.
- [17] Website: <https://www.ninds.nih.gov/Disorders/Patient-Caregiver-Education/Fact-Sheets/Cerebral-Aneurysms-Fact-Sheet> (access on 24th October 2021)